A mathematical model of α-catenin dimerization at Adherens Junctions in polarized epithelial cells

Adriana T. Dawes*,[1]

Center for Cell Dynamics, University of Washington, 620 University Rd., Friday Harbor, WA, 98250, USA

Abstract

The protein α-catenin is found as a monomer or homodimer. As a monomer, α-catenin can bind to β-catenin, which localizes to the plasma membrane at the site of Adherens Junctions (AJs) in polarized epithelial cells. As a dimer, α-catenin can bind to actin filaments, affecting the organization of the actin cytoskeleton. At usual cytoplasmic concentrations, α-catenin is found predominantly in monomeric form. It is currently thought that α-catenin can not simultaneously bind β-catenin and homodimerize, and that the dynamics of binding and unbinding from β-catenin, possibly coupled with lower diffusion near an AJ, are sufficient to locally accumulate α-catenin monomers and homodimers. Using a mathematical model of α-catenin dynamics, I show that α-catenin must transiently homodimerize while bound to β-catenin in order for homodimers to form, even in the presence of a spatial diffusion gradient.

Key words: Cell-cell adhesion, theoretical biology

1. Introduction

Sheets of multicellular tissues, such as epithelia that make up our skin and the lining of our lungs, are constructed and maintained by cell-cell adhesion (Ebnet, 2008). Cell adhesion is also important during embryonic development

*Corresponding author. Tel:780-492-3974, fax: 780-492-6826.
Email address: atdawes@math.ualberta.ca
[1]Present address: Department of Mathematical and Statistical Sciences, University of Alberta, Edmonton, AB, T6G 2G1, Canada

as cells join together and organize into different tissue types (Gumbiner, 2005). Cell adhesion is mediated by adhesion complexes that span the plasma membrane and have both intra- and extra-cellular components (Knust and Bossinger, 2002). These complexes are dynamic and constantly remodeling in response to changes in the cellular environment (Ebnet, 2008; Mège et al., 2006). Defects in cell adhesion can have grave consequences, and are implicated in metastatic cancer and embryonic defects (Kametani and Takeichi, 2007; Benjamin and Nelson, 2008; Hirohashi and Kanai, 2003). Epithelial cells which are polarized along the apical/basal axis (Wang and Margolis, 2007; Nelson, 2003) possess a particular type of adhesion complex referred to as Adherens Junctions (AJs), which consist of the proteins E-cadherin, β-catenin and α-catenin (Knust and Bossinger, 2002; D'Souza-Schorey, 2005), shown schematically in Figure 1.

E-cadherin is a transmembrane protein whose extracellular domain binds to E-cadherin on neighboring cells. The intracellular domain of E-cadherin strongly binds to β-catenin, a cytoplasmic protein, forming a stable complex. α-catenin, a cytoplasmic protein that is capable of homodimerizing, binds to β-catenin to form the AJ (Drees et al., 2005; Gumbiner, 2005; Niessen and Gottardi, 2008). Both α- and β-catenin are coiled-coil proteins, meaning their binding domains are composed of α helices. These are secondary protein structures where the amino acids are arranged in a helical configuration with every seventh amino acid lining up along the side of the helix (heptad repeat). The order of the amino acids determines various properties of the protein, including binding affinities. The α helices of α- and β-catenin entwine with each other to form a dimer.

AJs are found on the lateral sides of polarized epithelial cells near the apical surface and colocalize with the boundary between the biochemically distinct apical and basolateral domains (Ebnet et al., 2008; Nelson, 2003). In the cytoplasm, α-catenin is predominantly a monomer, constituting 60-75% of cytosolic α-catenin at a concentration of approximately 0.6 μM (Drees et al., 2005). The relative proportion of homodimers to monomers increases as the concentration

of α-catenin increases (Drees et al., 2005).

It has long been believed that α-catenin directly binds β-catenin and F-actin, stabilizing and anchoring AJs and the cytoskeleton (Gates and Peifer, 2005; Takeichi and Abe, 2005), based on the fact that the amino acid sequences corresponding to these functions do not overlap (Pokutta and Weis, 2000). However, recent work has demonstrated that α-catenin preferentially binds β-catenin as a monomer and binds F-actin as a dimer (Drees et al., 2005), and that α-catenin does not simultaneously bind F-actin and β-catenin in the AJ (Yamada et al., 2005; Miyoshi and Takai, 2008). It is also believed that α-catenin can not homodimerize while bound to β-catenin since the amino acid sequences corresponding to these two functions overlap (Koslov et al., 1997). As a result of these new findings, it was suggested that dissociation of α-catenin monomers from β-catenin at AJs, possibly coupled with a zone of decreased diffusion near an AJ, will generate a high local concentration of monomers and favor the formation of α-catenin homodimers (Weis and Nelson, 2006), shown schematically in Figure 1.

In this paper, I use mathematical modeling to directly test the assumption that dissociation of α-catenin monomers from AJs leads to a local accumulation of monomers and increased homodimer concentration. I construct the model using experimentally determined interactions and use parameter values derived from experimental data. I find that α-catenin association with AJs will not increase the local cytoplasmic concentration of monomers, and a local increase in homodimer concentration will occur only if α-catenin can homodimerize while bound to β-catenin, even with decreased diffusion near the AJ. It is currently thought that α-catenin homodimerization occurs as the sequence of events shown in Figure 2: α-catenin monomers dissociate from an E-cadherin/β-catenin complex at an AJ then bind together to form a homodimer. I propose that α-catenin homodimerization while bound to β-catenin may occur as a result of the amino acid configuration in the α-helices, allowing for the transient

formation of an α/β-catenin oligomer (Figure 3). Alternatively, α-catenin homodimerization while bound to β-catenin may occur through the association of a weak homodimerization domain that is disjoint from the β-catenin binding domain (Figure 4).

The proper dynamics, configuration (monomer or homodimer) and spatial localization of α-catenin at AJs are crucial for the functioning and maintenance of polarized domains in epithelial cells. However, there is a great deal that remains unknown about the formation and maintenance of AJs in polarized epithelial cells. Using mathematical modeling to explore the dynamics of components found in AJs may help shed light on how the individual kinetics of these molecules give rise to stable but dynamic cell-cell adhesion that is crucial for proper health and development in multicellular organisms.

2. The mathematical model

2.1. Model assumptions

A number of assumptions, based on experimental observations, were made in constructing this model of α-catenin binding and homodimerization.

1. Only α-catenin monomers, not homodimers, can bind to β-catenin, and α-catenin homodimers that are formed while bound to β-catenin immediately dissociate from β-catenin (Gates and Peifer, 2005; Koslov et al., 1997; Drees et al., 2005; Pokutta and Weis, 2000).
2. The number of β-catenin monomers available to bind α-catenin monomers is not limiting.
3. The complex of β-catenin and E-cadherin is stable compared to the association/dissociation kinetics of α-catenin (Drees et al., 2005).
4. α-catenin monomers and homodimers freely diffuse in the cytoplasm.
5. Cytoplasmic diffusion rates may decrease near an AJ, due to increased crowding of molecules, the presence of the actin belt and/or other factors (García-Pérez et al., 1999; Dix and Verkman, 2008; Banks and Fradin, 2005; Konopka et al., 2006).

6. α-catenin bound to β-catenin diffuses along the membrane at a very slow rate (approximately 0.005 μm^2/s, Kametani and Takeichi (2007)) and can be ignored here.
7. All interactions, such as homodimerization and binding, are direct and can be modeled using first order linear and mass action kinetics (Gates and Peifer, 2005).
8. AJs are localized structures that are relatively stable (Assumption 6). Assuming that AJs have a nonzero width and the distribution of E-cadherin and β-catenin within the AJ is homogeneous, the model equations can be simulated in 1D, representing a transect of the cell. The transect is perpendicular to the membrane, positioned in the middle of the AJ far from its edges, with the membrane located at $x = 0$ and the interior of the cell located at $x = +\infty$ (Figure 1).

2.2. Model variables

The mathematical model keeps track of three variables that change in time and space:

$A_m(x,t)$	cytoplasmic α-catenin monomers
$A_d(x,t)$	cytoplasmic α-catenin homodimers
$A_b(t)$	AJ bound α-catenin

2.3. Model equations

Based on experimental data concerning α-catenin dynamics and incorporating the assumptions listed above, the model equations describing α-catenin dynamics are:

$$\frac{\partial A_m}{\partial t} = \frac{\partial}{\partial x}\left(D_m(x)\frac{\partial A_m}{\partial x}\right) + I_{Am} - \delta_{Am}A_m - k_{df}^{+}A_m^2 + k_{df}^{-}A_d \quad (1a)$$

$$\frac{\partial A_d}{\partial t} = \frac{\partial}{\partial x}\left(D_d(x)\frac{\partial A_d}{\partial x}\right) + k_{df}^{+}A_m^2 - k_{df}^{-}A_d \quad (1b)$$

$$\frac{dA_b}{dt} = k_{on}A_m(0) - k_{off}A_b - k_{db}^{+}A_b^2 \quad (1c)$$

Equation 1a describes the dynamics of the cytoplasmic α-catenin monomer concentration. Monomers diffuse at a rate that may depend on space (Assumption

5), and are produced and lost through decay or dimerization. Similarly, Equation 1b, which describes the dynamics of the cytoplasmic α-catenin dimer concentration, incorporates a space dependent diffusion rate and production and loss by dimerization. The model is insensitive to the exact form of $D_m(x)$ and $D_c(x)$ and in the results discussed here, I assume it can be modeled using a Hill function. Equation 1c describes the temporal dynamics of α-catenin monomers bound to β-catenin at the AJ. Since we are ignoring diffusion of the E-cadherin/β-catenin complex along the membrane (Assumption 6), the bound monomers vary only in time and are gained through association from the cytoplasmic monomer pool and lost through dissociation or dimer formation.

The corresponding boundary conditions are:

$$-D_m \frac{\partial A_m}{\partial x}\bigg|_{x=0} = (-k_{on}A_m(0) + k_{off}A_b)/\eta \tag{2a}$$

$$-D_d \frac{\partial A_d}{\partial x}\bigg|_{x=0} = (k_{db}^{+}A_b^2)/\eta \tag{2b}$$

$$\frac{\partial A_m}{\partial x}\bigg|_{x=\infty} = 0 \tag{2c}$$

$$\frac{\partial A_d}{\partial x}\bigg|_{x=\infty} = 0 \tag{2d}$$

Equations 2a and 2b track the flux of α-catenin monomers and dimers at the AJ: monomers are lost and gained by binding and unbinding to β-catenin, while dimers are gained through homodimerization of bound monomers. The density of α-catenin binding sites on the membrane is denoted by η. Once a homodimer is formed, it immediately dissociates from the AJ (Assumption 1). Equations 2c and 2d impose no flux boundary conditions on α-catenin monomers and homodimers far from the membrane.

2.4. Parameter values

A number of parameter values for this system have already been determined. It is known that the approximate background concentration of α-catenin in the

cell is A_0=0.6 μm (Drees et al., 2005). To determine cytoplasmic diffusion coefficients, note that actin monomers, which have an approximate molecular weight of 40 kDa, have been demonstrated to have an approximate cytoplasmic diffusion rate of 5 μm^2/s (Dawes et al., 2006). Using the Stokes-Einstein relation and the estimate that α-catenin has a molecular weight of approximately 100 kDa (Kobielak and Fuchs, 2004) (and assuming α-catenin dimers have double that molecular weight), we can estimate the baseline diffusion coefficient of α-catenin monomers as D_{m0}=3.7 μm^2/s and dimers as D_{d0}=3.0 μm^2/s.

If we assume diffusion dominates over cytoplasmic production of α-catenin, we find $I_{Am} = 12\mu$M/s (discussed further in Appendix A) and in order to maintain a cytoplasmic concentration of A_0=0.6 μm, we must have $\delta_{Am} = 20\text{s}^{-1}$. The rate of α-catenin dimer formation has not yet been determined but is described as "rapid" (Drees et al., 2005), suggesting the rate of homodimer formation in the cytoplasm is $k_{df}^{+} = 10 - 100\text{s}^{-1}\mu\text{M}^{-1}$. Using a simple model of dimerization discussed in Appendix A, the homodimer dissociation rate is estimated as k_{df}^{-}=20 - 200s^{-1}. I assume the rate of homodimer formation among bound α-catenin monomers is the same as the rate for free monomers, $k_{db}^{+} = k_{df}^{+}$. The rate of α-catenin association (k_{on}=0.2 s^{-1}) and dissociation (k_{off}=0.005 s^{-1}) with β-catenin at the area of cell-cell contact can be determined using FRAP and FLIP data, as discussed in Appendix A. The density of α-catenin binding sites, $\eta = 62.5 - 400\mu\text{m}^{-2}$, is also discussed in Appendix A.

The parameter values, compiled in Table 1, are given in terms of concentrations. However, since there is binding and interactions between both cytoplasmic and membrane bound components, the model must use a volume conversion term or track interactions in terms of number of molecules instead of concentrations. For simplicity, and since the relative volume of the cytoplasmic and membrane compartments is not known, I chose to track the total number of molecules. An epithelial cell has an approximate volume of V=10^3 μm^3 (Fisher et al., 1981), or equivalently, $V = 10 \times 10^{-12}$ L/cell. Since 1 μM = 6.022 $\times 10^{17}$

molecules/L, we have the conversion factor for epithelial cells:

$$1\mu\text{M} = 6.022 \times 10^6 \text{molecules/cell}.$$

Discretization and simulation procedures are discussed in Appendix B and all simulations were performed with the converted rate constants.

3. Results

3.1. α-catenin dimer concentration will not increase above baseline if α-catenin can not dimerize while bound to β-catenin

Consider Equation 1 at steady state, with no homodimerization ($k_{df}^+ = k_{db}^+ = 0$) and with constant diffusion ($D_m(x) = D_{m0}$, $D_d(x) = D_{d0}$). Under these conditions, it is possible to determine if the monomer pool will ever exceed the usual cytoplasmic concentration, since there is no loss from the monomer pool due to homodimerization. At steady state, the resulting equations are:

$$D_m \frac{\partial^2 A_m}{\partial x^2} + I_{Am} - \delta_{Am} A_m = 0 \tag{3a}$$

$$k_{on} A_m(0) - k_{off} A_b = 0 \tag{3b}$$

$$\left.\frac{\partial A_m}{\partial x}\right|_{x=0,\infty} = 0 \tag{3c}$$

This system of equations has a unique analytic solution:

$$A_m(x) = \frac{I_{Am}}{\delta_{Am}}, \; A_b = \frac{k_{on} I_{Am}}{k_{off} \delta_{Am}}$$

shown in Figure 5A. In this case, the monomer concentration tends to its usual concentration everywhere in the cytoplasm and only the bound population of monomers achieves an elevated concentration. When Equations 1 are simulated numerically using $k_{df}^+ \neq 0$, $k_{db}^+ = 0$, both the monomer and homodimer concentrations tend to their usual levels (Figure 5B).

This suggests that β-catenin binding alone is insufficient to accumulate α-catenin monomers near an AJ to promote homodimer formation.

3.2. A spatial gradient of α-catenin dimers is seen when α-catenin dimerizes while bound to β-catenin

Consider Equations 1 with homodimerization of both free and bound α-catenin monomers ($k_{df}^{+} \neq 0$, $k_{db}^{+} \neq 0$) and with constant diffusion everywhere in the cytoplasm ($D_m(x) = D_{m0}$, $D_d(x) = D_{d0}$). Numerical simulations result in a spatial gradient of homodimers originating from the AJ, as shown in Figure 6. These results suggest that in the absence of a zone of decreased diffusion near an AJ, a spatial gradient of dimers near an AJ can be formed only when α-catenin can simultaneously dimerize while bound to β-catenin.

3.3. α-catenin dimers do not accumulate near an AJ in the presence of a diffusion gradient if α-catenin can not dimerize while bound to β-catenin

Next consider the case with a diffusion gradient near the AJ ($D_m(x)$, $D_d(x)$ not constant) and α-catenin homodimers can form only in the cytoplasm ($k_{df}^{+} \neq 0$, $k_{db}^{+} = 0$). A diffusion gradient is characterized by a decrease in the cytoplasmic diffusion rate near the location of an AJ (Assumption 5). Figure 7 shows some typical spatial profiles of diffusion gradients used in the simulations here.

When numerical simulations of Equations 1 in the presence of a diffusion gradient are performed, where α-catenin monomers are only allowed to dimerize in the cytoplasm, there is again no additional production of α-catenin homodimers above the usual cytoplasmic level, resulting in spatial profiles similar to those shown in Figure 5. This suggests that a diffusion gradient coupled with β-catenin binding is still insufficient to raise the cytoplasmic level of α-catenin monomers high enough for local accumulation of homodimers.

3.4. A diffusion gradient affects the spatial profile of α-catenin monomers and dimers when α-catenin can dimerize while bound to β-catenin

When all aspects of the model are combined together (diffusion gradient near the AJ, $D_m(x)$, $D_d(x)$ not constant, dimerization of cytoplasmic and bound monomers, $k_{df}^{+} \neq 0$, $k_{db}^{+} \neq 0$) and Equations 1 are simulated, the spatial profiles shown in Figure 8 are produced. These plots show the spatial distribution of α-catenin monomers and dimers in the presence of a diffusion gradient that

decreases diffusion by various amounts. A spatial gradient of α-catenin dimers near an AJ is seen only when α-catenin can dimerize while bound to β-catenin. A diffusion gradient near the AJ qualitatively modifies the spatial profile of both monomers and dimers, with a greater accumulation of α-catenin dimers near the AJ as the diffusion rate in the gradient decreases. These results indicate that it is crucial for α-catenin monomers to dimerize while bound to β-catenin at AJs, and a diffusion gradient near an AJ serves only to modify the spatial profile of α-catenin monomers and homodimers.

4. Discussion

The cadherin/catenin complex that localizes to AJs at cell-cell contacts is required for building and maintaining various types of multicellular tissues, including epithelia (Ebnet, 2008; Gumbiner, 2005; Knust and Bossinger, 2002). However, many details about how this complex is formed and stably maintained remain unclear. Recent work has demonstrated that α-catenin preferentially binds to β-catenin as a monomer, and binds to F-actin as a dimer to locally remodel the actin cytoskeleton (Drees et al., 2005). It has been suggested that exchange of α-catenin with its cytoplasmic pool in the vicinity of AJs will cause a local accumulation of α-catenin monomers which would favor the formation of α-catenin homodimers (Weis and Nelson, 2006). The mathematical model of α-catenin dynamics near an AJ developed and analyzed here argues against that scenario and indicates that association with an AJ does not promote a high local cytoplasmic concentration of monomers. Instead, the model results indicate that α-catenin homodimers will form only if dimerization can occur while α-catenin is bound to β-catenin. With this model, only a *de novo* source of α-catenin monomers at an AJ would allow for the accumulation of homodimers near an AJ if the monomers are unable to homodimerize while bound to β-catenin.

To understand why α-catenin binding to AJs does not lead to a local monomer accumulation, consider the flux of monomers at a stable AJ. It has been observed

that α-catenin monomers bound to AJs maintain a non-zero steady-state concentration (Miyoshi and Takai, 2008; D'Souza-Schorey, 2005). To maintain that concentration, the same number of α-catenin monomers must bind to the AJ as are released. Otherwise, if AJs bind more monomers than they release, the bound monomer concentration would continue to increase over time. Conversely, if less monomers bind than are released, the bound monomer concentration would decay to zero, provided there was an initial bound population. In other words, a stable AJ must continually bind as many α-catenin monomers from the cytoplasm to replace monomers that unbind, resulting in a zero net flux of monomers. Without a source of α-catenin monomers at an AJ, binding kinetics can not lead to a local accumulation of α-catenin monomers sufficient to promote homodimerization, even in the presence of a spatial diffusion gradient. It has long been assumed that α-catenin homodimerization and binding to β-catenin are mutually exclusive since the sequence domains corresponding to these functions overlap (residues 82-279 and 54-148, respectively, Koslov et al. (1997); Kobielak and Fuchs (2004)). However, I propose two possible mechanisms that may allow α-catenin to dimerize while bound to β-catenin.

The first mechanism, shown schematically in Figure 3, relies on thermal fluctuations of neighboring α-catenin monomers bound to β-catenin, and the structure of the coiled-coil domains of α and β-catenin. The wheel diagram, Figure 9, shows the amino acid arrangement of α-catenin bound to β-catenin, with hydrophobic amino acids shown in red. Under the "Peptide Velcro" hypothesis, hydrophobic interactions between amino acid residues at the a and d positions coupled with charged residues at the e and g positions stabilize a dimer (Mason and Arndt, 2004). Clearly the residues at the e and g positions corresponding to the α2 helix of α-catenin are hydrophobic and do not meet these requirements, making the α/β-catenin dimer unstable. With this α/β-catenin dimer instability, it is possible that thermal fluctuations of neighboring α-catenins bound to β-catenin could expose the homodimerization domain, allowing for the transient formation of a $\beta/\alpha/\alpha/\beta$-catenin oligomer. The α-catenin homodimer thus

formed would rapidly dissociate from β-catenin and diffuse into the cytoplasm. It may be possible to test this mechanism experimentally by altering the amino acid sequence in the $\alpha 2$ helix of α-catenin so that the e and g residues are either hydrophilic or charged to form a more stable α/β-catenin dimer. The model predicts a decrease in α-catenin homodimer formation under those conditions.

The second mechanism (Figure 4) relies on the M fragment of α-catenin (residues 377-633), which is a sequence disjoint from the homodimerization and β-catenin binding domains, and which can weakly homodimerize (Yang et al., 2001; Imamura et al., 1999). It may be possible for a weak α-catenin homodimer to form through M fragment association while monomers are bound to β-catenin. This weak homodimer would dissociate from β-catenin, exposing the strong homodimerization domain. There is experimental support for this mechanism, as adhesion is weak when the M fragment is missing, which was thought to result from the absence of actin-based interactions modulated by the M fragment. However, recent work shows that α-catenin does not simultaneously bind β-catenin and F-actin (Yamada et al., 2005). The model analyzed here suggests a possible alternate function for α-catenin's M fragment: it transiently homodimerizes α-catenin while it is bound to β-catenin which could cause cells that express α-catenin with a non-functional M fragment to show weak adhesion due to lack of homodimer formation. This mechanism can be tested experimentally using cells expressing GFP-α-catenin with a non-functional M fragment. According to the model predictions, the spatial profiles of α-catenin monomers and homodimers should appear similar to those in Figure 5, with no increased homodimer formation near an AJ.

Regardless of the mechanism for homodimerization, the model results suggest a possible sequence of events that agree with experimental findings of Yamada et al. (2005) and Drees et al. (2005). α-catenin monomers diffuse past actin filaments due to low binding affinity and eventually reach an AJ at the membrane where they bind to a β-catenin/E-cadherin complex. Pairs of bound

α-catenin monomers are brought into close physical proximity due to homodimerization and clustering of E-cadherin at AJs (Pertz et al., 1999; Troyanovsky et al., 2007). While bound to β-catenin, α-catenin pairs form homodimers, which then quickly dissociate due to a lowered binding affinity. The α-catenin dimers do not rebind to β-catenin but diffuse away from the membrane to associate with actin filaments to regulate filament assembly.

The model developed here is generic and the mechanism may be applicable to other molecules that require a higher local concentration and specific localization for activation, dimerization or other activity. As mentioned, in this model only *de novo* production of α-catenin monomers at an AJ would raise the local concentration of homodimers. Since this is not biologically reasonable, this makes the model robust to both changes in the form of the model and variations in parameter values. Changing the form of the model, including modifying the spatial dependence of the diffusion coefficients, does not change the flux of monomers at the membrane: the E-cadherin/β-catenin complex must still bind as many monomers as it releases to maintain a steady-state concentration, resulting in zero net flux of monomers. Variations in parameter values will also not change the qualitative properties of the model, only quantitatively modify the spatial profiles. However, this model does not take into account other processes such as non-specific binding to other proteins near an AJ that could be responsible for accumulation of α-catenin monomers. The model discussed here was investigated using a simplified 1D geometry. Extending the simulations to 2D or 3D does not alter any of the results discussed here and provides a simulation framework for future extensions of this work, including explorations of AJ formation and actin filament reorganization.

Cell-cell adhesion mediated by AJs is an important biological phenomenon and many aspects of AJ activity remain unclear. Further work, both experimentally and theoretically, is needed to continue untangling the activity and localization of components in AJs.

Acknowledgments

The author thanks Dr. W. James Nelson, Dr. Leah Edelstein-Keshet and members of the Center for Cell Dynamics, especially Dr. Yvonne Beckham, for helpful discussions and critical reading of the manuscript. This work was supported by the NIGMS 5P50 GM66050-02 grant to Dr. G. M. Odell, Center for Cell Dynamics, University of Washington.

References

Banks, D., Fradin, C., 2005. Anomalous diffusion of proteins due to molecular crowding. Biophysical Journal 89 (5), 2960–2971.

Benjamin, J., Nelson, W., 2008. Bench to bedside and back again: molecular mechanisms of alpha-catenin function and roles in tumorigenesis. Seminars in Cancer Biology 18 (1), 53–64.

Dawes, A. T., Ermentrout, G. B., Cytrynbaum, E. N., Edelstein-Keshet, L., 2006. Actin filament branching and protrusion velocity in a simple 1D model of a motile cell. Journal of Theoretical Biology 242 (2), 265–279.

Dix, J., Verkman, A., 2008. Crowding effects on diffusion in solutions and cells. Annual Review of Biophysics 37, 247–263.

Drees, F., Pokutta, S., Yamada, S., Nelson, W., Weis, W., 2005. alpha-catenin is a molecular switch that binds E-cadherin-beta-catenin and regulates actin-filament assembly. Cell 123 (5), 903–915.

D'Souza-Schorey, C., 2005. Disassembling adherens junctions: breaking up is hard to do. Trends in Cell Biology 15 (1), 19–26.

Duguay, D., Foty, R., Steinberg, M., 2003. Cadherin-mediated cell adhesion and tissue segregation: qualitative and quantitative determinants. Developmental Biology 253 (2), 309–323.

Ebnet, K., 2008. Organization of multiprotein complexes at cell-cell junctions. Histochemistry and Cell Biology 130 (1), 1–20.

Ebnet, K., Iden, S., Gerke, V., Suzuki, A., 2008. Regulation of epithelial and endothelial junctions by PAR proteins. Frontiers in Bioscience 13, 6520 – 6536.

Fisher, R., Persson, B., Spring, K., 1981. Epithelial cell volume regulation: bicarbonate dependence. Science 214 (4527), 1357–1359.

García-Pérez, A., López-Beltrán, E., Klüner, P., Luque, J., Ballesteros, P., Cerdán, S., 1999. Molecular crowding and viscosity as determinants of translational diffusion of metabolites in subcellular organelles. Archives of Biochemistry and Biophysics 362 (2), 329–338.

Gates, J., Peifer, M., 2005. Can 1000 reviews be wrong? Actin, alpha-Catenin, and adherens junctions. Cell 123 (5), 769–772.

Gumbiner, B., 2005. Regulation of cadherin-mediated adhesion in morphogenesis. Nature Reviews Molecular Cell Biology 6 (8), 622–634.

Hirohashi, S., Kanai, Y., 2003. Cell adhesion system and human cancer morphogenesis. Cancer Science 94 (7), 575–581.

Imamura, Y., Itoh, M., Maeno, Y., Tsukita, S., Nagafuchi, A., 1999. Functional domains of alpha-catenin required for the strong state of cadherin-based cell adhesion. Journal of Cell Biology 144 (6), 1311–1322.

Kametani, Y., Takeichi, M., 2007. Basal-to-apical cadherin flow at cell junctions. Nature Cell Biology 9 (1), 92–982.

Knust, E., Bossinger, O., 2002. Composition and formation of intercellular junctions in epithelial cells. Science 298 (5600), 1955–1959.

Kobielak, A., Fuchs, E., 2004. α-catenin: At the junction of intercellular adhesion and actin dynamics. Nature Reviews Molecular Cell Biology 5 (8), 614–625.

Konopka, M., Shkel, I., Cayley, S., Record, M., Weisshaar, J., 2006. Crowding and confinement effects on protein diffusion in vivo. Journal of Bacteriology 188 (17), 6115–6123.

Koslov, E., Maupin, P., Pradhan, D., Morrow, J., Rimm, D., 1997. Alpha-catenin can form asymmetric homodimeric complexes and/or heterodimeric complexes with beta-catenin. Journal of Biological Chemistry 272 (43), 27301–27306.

Mason, J., Arndt, K., 2004. Coiled coil domains: stability, specificity, and biological implications. ChemBioChem 5 (2), 170–176.

Mège, R., Gavard, J., Lambert, M., 2006. Regulation of cell-cell junctions by the cytoskeleton. Current Opinion in Cell Biology 18 (5), 451–548.

Miyoshi, J., Takai, Y., 2008. Structural and functional associations of apical junctions with cytoskeleton. Biochimica et Biophysica Acta (BBA) - Biomembranes 1778 (3), 670–691.

Nelson, W., 2003. Adaptation of core mechanisms to generate cell polarity. Nature 422 (6933), 766–74.

Niessen, C., Gottardi, C., 2008. Molecular components of the adherens junction. Biochimica et Biophysica Acta (BBA) - Biomembranes 1778 (3), 562–571.

Perez, T., Tamada, M., Sheetz, M., Nelson, W., 2008. Immediate-early signaling induced by E-cadherin engagement and adhesion. Journal of Biological Chemistry 283 (8), 5014–5022.

Pertz, O., Bozic, D., Koch, A., Fauser, C., Brancaccio, A., Engel, J., 1999. A new crystal structure, Ca2+ dependence and mutational analysis reveal molecular details of E-cadherin homoassociation. EMBO Journal 18 (7), 1738–1747.

Pokutta, S., Weis, W., 2000. Structure of the dimerization and beta-catenin-binding region of alpha-catenin. Molecular Cell 5 (3), 533–543.

Press, W., Flannery, B., Teukolsky, S., Vetterling, W., 2002. Numerical Recipes in C: The Art of Scientific Computing, 2nd Edition. Cambridge University Press.

Takeichi, M., Abe, K., 2005. Synaptic contact dynamics controlled by cadherin and catenins. Trends in Cell Biology 15 (4), 216–221.

Troyanovsky, R., Laur, O., Troyanovsky, S., 2007. Stable and unstable cadherin dimers: mechanisms of formation and roles in cell adhesion. Molecular Biology of the Cell 18 (11), 43434–43452.

Wang, Q., Margolis, B., 2007. Apical junctional complexes and cell polarity. Kidney International 72 (12), 1448–1458.

Weis, W., Nelson, W., 2006. Re-solving the cadherin-catenin-actin conundrum. Journal of Biological Chemistry 281 (47), 35593–35597.

Yamada, S., Pokutta, S., Drees, F., Weis, W., Nelson, W., 2005. Deconstructing the cadherin-catenin-actin complex. Cell 123 (5), 889–901.

Yang, J., Dokurno, P., Tonks, N., Barford, D., 2001. Crystal structure of the M-fragment of alpha-catenin: implications for modulation of cell adhesion. EMBO Journal 20 (14), 3645–3656.

A. Determination of parameter values

As discussed in Section 2.4, a number of parameter values for this system are found in the experimental literature. However, the rate of α-catenin binding and unbinding from β-catenin at AJs, as well as the rate of cytosolic α-catenin production and decay, are not currently known. Here, I use simple models with experimental data to determine approximate values for these unknown parameters.

A.1. Cortical association and dissociation rates of monomeric α-catenin

To estimate α-catenin binding and unbinding rates, I use FLIP (Fluorescence Loss In Photobleaching) data from Drees et al. (2005) and FRAP (Fluorescence Recovery After Photobleaching) data from Yamada et al. (2005), along with a simple model of photobleached and fluorescent α-catenin. This simple model ignores cytoplasmic production and decay of GFP-α-catenin, as well as lateral diffusion of bound GFP-α-catenin in AJs. The cytoplasm is assumed to be well-mixed, allowing diffusion to be ignored. I also assume the total amounts of cytoplasmic GFP-α-catenin (A_{mT}) and β-catenin bound GFP-α-catenin (A_{bT}) are conserved.

In FLIP experiments, a portion of the cytoplasm is photobleached and the corresponding loss of fluorescence in both the cytoplasm and the membrane is observed. By conservation, we only need to consider the dynamics of the unbleached cytoplasmic (A_m) and AJ-associated (A_b) α-catenin monomers. The equations are:

$$\frac{dA_m}{dt} = -\overline{r_b}A_m \tag{4a}$$

$$\frac{dA_b}{dt} = \overline{k_{on}}A_m - \overline{k_{off}}A_b \tag{4b}$$

Since fluorescence is reported in dimensionless intensity units, Equations 4 must be scaled. Let $\overline{A_m}$ be the characteristic (dimensional) scale of the unbleached cytoplasmic monomer concentration and let A_m^* be the dimensionless variable, such that $A_m = \overline{A_m} \cdot A_m^*$, and similarly for A_b. The scaled equations are then:

$$\frac{dA_m^*}{dt} = -r_b A_m^* \tag{5a}$$

$$\frac{dA_b^*}{dt} = k_{on}A_m^* - k_{off}A_b^* \tag{5b}$$

where $r_b = \overline{r_b}$, $k_{off} = \overline{k_{off}}$, $k_{on} = \overline{k_{on}}\,\overline{A_m}/\overline{A_b}$.

Equation 5a can be solved explicitly:

$$A_m^*(t) = e^{-r_b t}$$

where $A_m^*(0) = 1$ before photobleaching. We can fit this equation to the FLIP data presented in Figure 4E of Drees et al. (2005), giving the value

$$r_b \approx 0.74\text{min}^{-1}.$$

The analytic expression for A_m^* can be substituted into Equation 5b, which can also be solved explicitly:

$$A_b^*(t) = \frac{k_{on}}{k_{off} - r_b} e^{-r_b t} + \left(1 - \frac{k_{on}}{k_{off} - r_b}\right) e^{-k_{off} t} \tag{6}$$

using $A_b^*(0) = 1$. As indicated in Figure 4E of Drees et al. (2005), the fluorescence level on the membrane decreases by approximately 10% over 9 minutes, making $A_b^*(9) \approx 0.9 A_b^*(0)$, which can be substituted into Equation 6 and rearranged into an explicit expression for k_{on} in terms of k_{off}:

$$k_{on} = \frac{(0.9 - e^{-9k_{off}})(k_{off} - r_b)}{e^{-9r_b} - e^{-9k_{off}}}. \tag{7}$$

FRAP data from Yamada et al. (2005), where a portion of the cell-cell contact area is photobleached and the subsequent fluorescence recovery is observed, suggests the half-time of fluorescence recovery for GFP-α-catenin in AJs is approximately 0.43 minutes. Using Equation 5b but assuming the pool of unbleached α-catenin monomers is unaffected by the small number of photobleached monomers unbinding from AJs so that $A_m^*(t) = 1$, we find the following explicit expression for $A_b^*(t)$:

$$A_b^*(t) = \frac{k_{on}}{k_{off}} \left(1 - e^{-k_{off} t}\right) \tag{8}$$

where $A_b^*(0) = 1$ before photobleaching. Using $A_b^*(0.43) = 0.5 A_b^*(0)$ and rearranging the equation, we arrive at another expression for k_{on}:

$$k_{on} = \frac{0.5 k_{off}}{1 - e^{-0.43 k_{off}}} \tag{9}$$

Simultaneously solving Equations 7 and 9, we find

$$k_{on} = 1.2\text{min}^{-1} \tag{10a}$$

$$k_{off} = 0.13\text{min}^{-1} \tag{10b}$$

Converting these to dimensional parameters for use in simulations,

$$\overline{r_b} = 0.74\text{min}^{-1} \tag{11a}$$

$$\overline{k_{off}} = 0.13\text{min}^{-1} \tag{11b}$$

$$\overline{k_{on}} = 12\text{min}^{-1} \tag{11c}$$

where I assumed $\overline{A_b} \approx 10\overline{A_m}$, since the concentration of α-catenin monomers at AJs is much higher than the cytoplasmic concentration (Imamura et al., 1999; Kobielak and Fuchs, 2004; Weis and Nelson, 2006).

A.2. Cytoplasmic production and decay rates of monomeric α-catenin

To determine approximate cytoplasmic source and decay rates for α-catenin monomers, I assume that diffusion from and to other parts of the cell would act faster than *de novo* production and decay of α-catenin, so that the monomer source term used here reflects redistribution by diffusion. While the *de novo* production of α-catenin monomers is likely not constant in space, I assume it is not spatially coincident with an AJ and therefore does not interfere with the flux of monomers at an AJ. In addition, redistribution of monomers by diffusion will dominate over *de novo* production further smoothing any spatial inhomogeneities in monomer production. The maximum "source" rate due to diffusion can be determined by considering a cube with 1 μm edge length that is initially empty and surrounded by a pool of α-catenin monomers at concentration A_0=0.6 μM. If monomers are allowed to diffuse into the empty cube at the rate D_{m0} (and assuming monomers are prevented from diffusing back out) and assuming the monomer pool outside the cube does not get depleted, the source rate of α-catenin monomers across all six faces is:

$$I_{Am} = 6\frac{D_{m0}A_0}{1\mu\text{m}^2} \approx 12\mu\text{M/s}. \tag{12}$$

In order to maintain a steady state cytoplasmic concentration of A_0, the decay rate must be:

$$\delta_{Am} = \frac{I_{Am}}{A_0} \approx 20\text{s}^{-1}. \tag{13}$$

A.3. α-catenin homodimerization and dissociation rates

I use a simple model of α-catenin dimerization in the cytoplasm to determine approximate kinetic rates for dimer formation and dissociation. I ignore spatial variation and consider only temporal dynamics, and ignore all terms except those involved with dimerization. I further assume the total amount of α-catenin (A_T) is conserved, leading to the following model:

$$\frac{dA_m}{dt} = -k_{df}^{+}A_m^2 + k_{df}^{-}A_d \tag{14a}$$

$$\frac{dA_d}{dt} = k_{df}^{+}A_m^2 - k_{df}^{-}A_d \tag{14b}$$

At steady state, $\frac{dA_d}{dt} = 0 \Rightarrow A_d = \frac{k_{df}^{+}A_m^2}{k_{df}^{-}}$. By conservation, $A_T = A_m + A_d \Rightarrow A_m = A_T - A_d$, and thus

$$A_d = \frac{k_{df}^{+}A_m(A_T - A_d)}{k_{df}^{-}} \tag{15a}$$

$$\Rightarrow \frac{A_d}{A_T} = \frac{A_m}{k_{df}^{-}/k_{df}^{+} + A_m} \tag{15b}$$

This relation tells us the proportion of homodimers we have as a function of the concentration of α-catenin monomers. If we choose the half maximal concentration $k_{df}^{-}/k_{df}^{+} = 2\mu$M, then at a monomer concentration of 0.6 μM, the usual cytoplasmic level, approximately 23% of the total α-catenin concentration will be in dimer form, while raising the monomer concentration to 6 μM will lead to 75% of the total concentration in dimer form, in agreement with experimental observations (Drees et al., 2005).

A.4. Density of α-catenin binding sites on the membrane

The parameter η is the ratio of the number of α-catenin binding sites per μm^2 of membrane. This factor is required in the boundary conditions (Equations 2) as α-catenin associates and dissociates from the E-cadherin/β-catenin complex. The surface density of E-cadherin has been estimated as 2.5 - 16 $\times 10^4$ molecules per cell (Duguay et al., 2003). Using a cell surface area of 400 μm^2 (Perez et al.,

2008), and assuming that each E-cadherin binds to one β-catenin molecule and is available for binding to α-catenin, then

$$\eta = \frac{2.5 - 16 \times 10^4 \text{ binding sites/cell}}{400\ \mu\text{m}^2/\text{cell}} \tag{16a}$$

$$= 62.5 - 400 \text{ binding sites}/\mu\text{m}^2 \tag{16b}$$

A.5. Sensitivity to parameter values

The model results are not sensitive to the exact choice of parameter values and the model behavior is not qualitatively altered by varying any of the parameters by several orders of magnitude. The model results are insensitive to the exact form of the spatial dependence of the diffusion coefficients, as this does not affect the flux of monomers at the AJ. The model results are also insensitive to small spatial variations in the rate of monomer production since cytoplasmic diffusion is relatively fast ($\sim$3 μm^2/s) and would smooth out any spatial variation in monomer concentration. The only instance where the model would be significantly affected by spatial variation of monomer production is if monomers were produced only at or near the site of an AJ. In that case, there would be a flux of monomers into the cell, producing a spatial gradient and the possibility of increased homodimer production. However, it is not biologically reasonable that monomers would be produced only at spatial locations coincident with AJs and I do not consider that possibility here.

B. Discretization and numerical simulations

For numerical simulations, Equations 1 were discretized on a one-dimensional domain with the appropriate boundary conditions using the Forward Time Centered Space (FTCS) (in the case of constant diffusion) and a modified FTCS for the case of non-constant diffusion, as discussed in Press et al. (2002). Initially all values were set to their usual cytoplasmic levels everywhere on the domain, as discussed in Section 2.4. The discretized equations were coded using the C programming language and simulated on a 10 μm grid with a space step size of 0.01 μm. The time step size was chosen for numerical stability. Simulations were run until the system achieved steady state.

Table legends

Table 1: Parameters used in the models discussed here.

Figure legends

Figure 1: Schematic of polarized epithelial cell and molecular components that make up adherens junctions (AJs). β-catenin is localized to AJs by binding to the transmembrane protein E-cadherin. The E-cadherin/β-catenin complex (red rectangle) has both intracellular and extracellular domains and crosses the membrane (thick vertical line). There is a zone of decreased diffusion near the membrane (grey area), which may be the result of crowding or non-specific binding. α-catenin monomers (green) bind to β-catenin with high affinity while α-catenin homodimers bind to polymerized actin with high affinity. In the cytoplasm, α-catenin is predominantly monomeric, suggesting the need for a mechanism to accumulate homodimers near AJs.

Figure 2: Sequence of events currently thought to lead to increased concentration of α-catenin homodimers near an AJ. A. α-catenin monomers (green) bind to β-catenin/E-cadherin (red) at an AJ. The plasma membrane is grey, and here the outside of the cell is below the membrane. B. α-catenin monomers are released from the AJ and diffuse into the cytoplasm. C. α-catenin monomers bind to form a homodimer that diffuses into the cell.

Figure 3: First possible mechanism for α-catenin homodimerization while bound to β-catenin. α-catenin, β-catenin/E-cadherin and the membrane are as described in Figure 2. A. α-catenin monomers are bound to β-catenin/E-cadherin at an AJ. B. Homodimerization of E-cadherin brings α-catenin monomers into close proximity, and fluctuations in the position of α-catenin relative to β-catenin allows α-catenin to homodimerize while still bound to β-catenin. C.

The α-catenin homodimer dissociates from β-catenin and diffuses into the cell.

Figure 4: Second possible mechanism for α-catenin homodimerization while bound to β-catenin. α-catenin, β-catenin/E-cadherin and the membrane are as described in Figure 2. A. The M fragment of α-catenin monomers bound to β-catenin/E-cadherin weakly homodimerize. B. The weak α-catenin homodimer dissociates from β-catenin, allowing binding of the strong homodimerization domain. C. The weak homodimerization domain unbinds, and the strongly bound homodimer diffuses into the cell.

Figure 5: A) Analytic solution of Equation 3 at steady state and B) numeric solution of Equation 1 with constant diffusion and α-catenin homodimerization only in the cytoplasm, showing cytoplasmic monomer concentration (—), cytoplasmic dimer concentration ($\cdots$), and membrane bound monomer concentration ($\bullet$). When α-catenin bound to β-catenin can not homodimerize and there is no spatial diffusion gradient near the AJ, the cytoplasmic concentration of α-catenin monomers will never exceed the usual cytoplasmic concentration or increase the production of homodimers near an AJ.

Figure 6: Steady state solution of Equation 1 with constant diffusion and homodimerization of cytoplasmic and bound α-catenin monomers, showing A) cytoplasmic monomer concentration and B) cytoplasmic homodimer concentration. A spatial gradient of α-catenin dimers are found in the cytoplasm when monomers bound to β- catenin are allowed to dimerize.

Figure 7: Spatial profile of sample diffusion gradients, with the rate of monomer diffusion decreasing close to the membrane ($x = 0$). Shown here are diffusion gradients that decrease the usual diffusion rate to 1/10 within 0.2 μm of the membrane (—) and 1/100 the usual rate within 5 μm of the membrane ($\cdots$).

Figure 8: Numeric solution of Equations 1 in the presence of a diffusion gra-

dient when both bound and cytoplasmic α-catenin monomers can homodimerize, showing A) cytoplasmic monomer concentration and B) cytoplasmic dimer concentration (membrane-bound monomer concentration not shown). When α-catenin can dimerize while bound to β-catenin, the spatial profile of cytoplasmic monomers and dimers depends on the size of the diffusion gradient and how much it slows diffusion. Shown here is a diffusion gradient that extends 1 μm into the cell and decreases monomer diffusion by a factor of 2 (—), 10 ($\cdots$) and 100 ($- - -$).

Figure 9: Wheel diagram of the amino acid sequence in the α-helical coiled-coil domains of α- catenin bound to β-catenin. Shown here are the α0 (amino acids 59-81), α1 (89-116) and α2 (124-144) helices of α-catenin, which include both the β-catenin binding (54-143) and homodimerization (82-279) domains (Koslov et al., 1997; Kobielak and Fuchs, 2004; Pokutta and Weis, 2000), along with the α-catenin binding domain of β-catenin (118-141). Hydrophobic residues are shown in red. Hydrophobic residues at the e and g positions of the α2 helix of α-catenin suggest the α/β-catenin dimer is unstable.

Tables

Parameter	Meaning	Value	Reference
A_0	Cytoplasmic monomer concentration	0.6 μM	Drees et al. (2005)
D_{m0}	Monomer diffusion coefficient	3.7 $\mu m^2/s$	this paper
D_{d0}	Dimer diffusion coefficient	3.0 $\mu m^2/s$	this paper
I_{Am}	Rate of monomer production	12 μM/s	this paper
δ_{Am}	Rate of monomer decay	20 s^{-1}	this paper
k_{df}^+	Rate of cytoplasmic homodimer formation	10-100 $s^{-1}\mu M^{-1}$	Drees et al. (2005)
k_{df}^-	Rate of cytoplasmic homodimer dissociation	20-200 s^{-1}	this paper
k_{db}^+	Rate of bound homodimer formation	10-100 $s^{-1}\mu M^{-1}$	this paper
k_{on}	Rate of monomer binding at AJ	0.2 s^{-1}	Drees et al. (2005), Yamada et al. (2005), this paper
k_{off}	Rate of monomer dissociation from AJ	0.005 $^{-1}$	Drees et al. (2005), Yamada et al. (2005), this paper
η	Number of binding sites per μm^2 of membrane	62.5 - 400 μm^{-2}	this paper

Table 1:

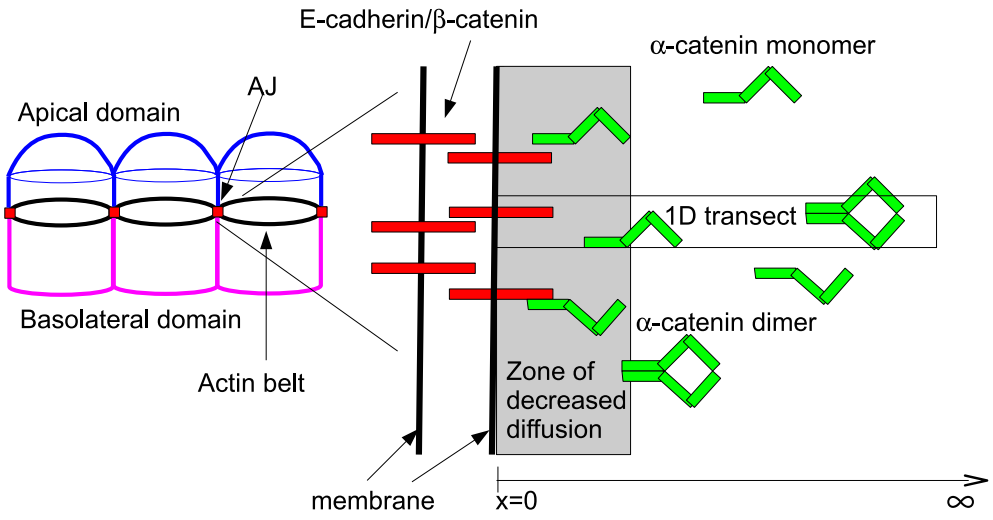

Figure 1:

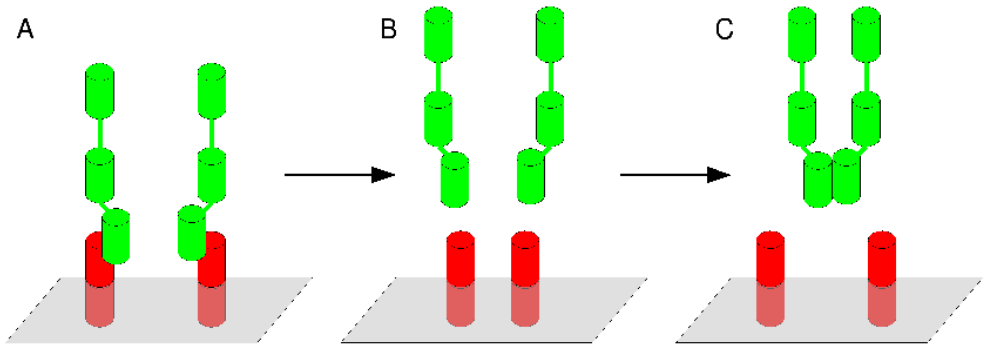

Figure 2:

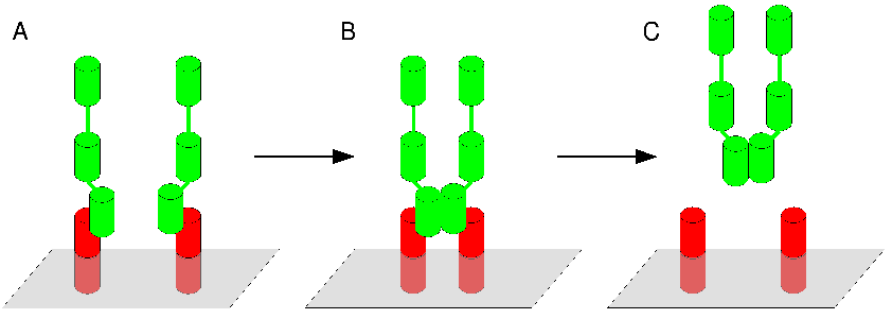

Figure 3:

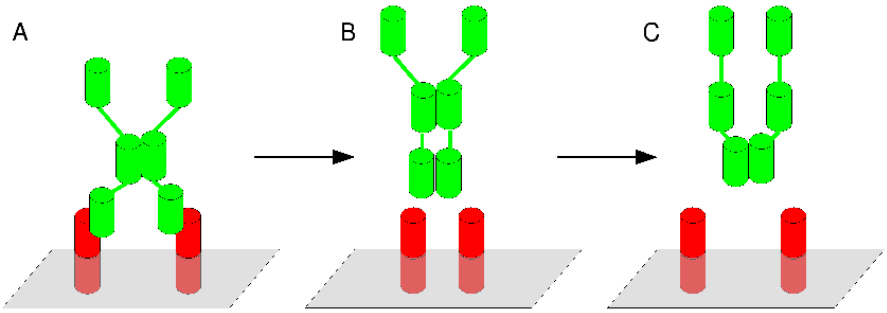

Figure 4:

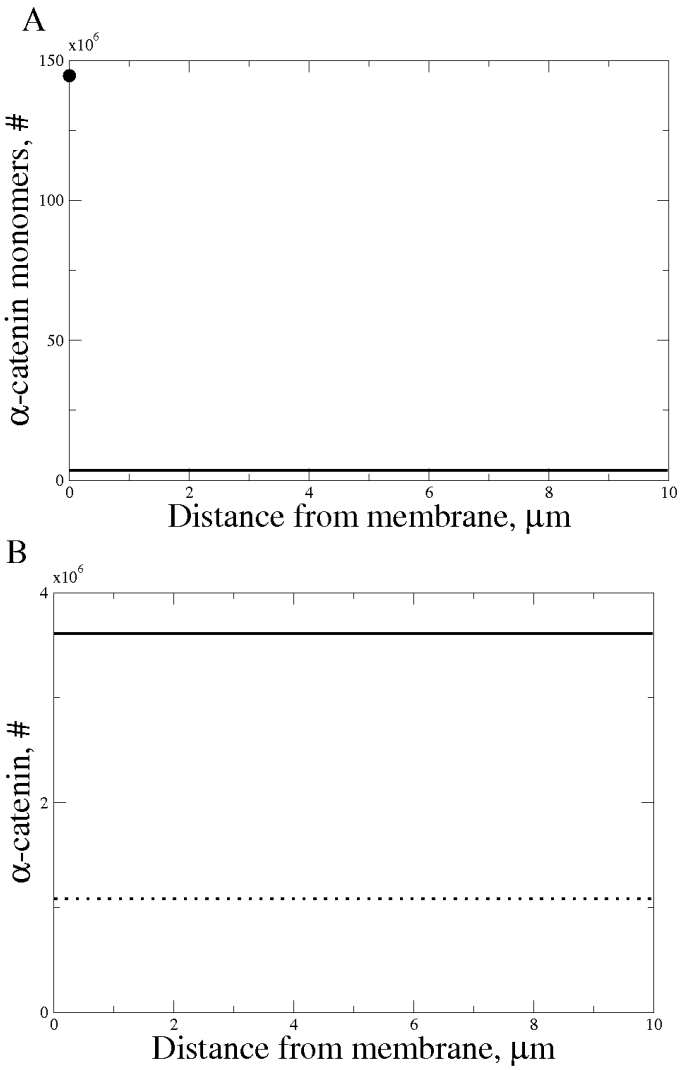
A
x10^6
150
100
50
0
α-catenin monomers, #
0
2
4
6
8
10
Distance from membrane, μm
B
x10^6
4
2
0
α-catenin, #
0
2
4
6
8
10
Distance from membrane, μm

Figure 5:

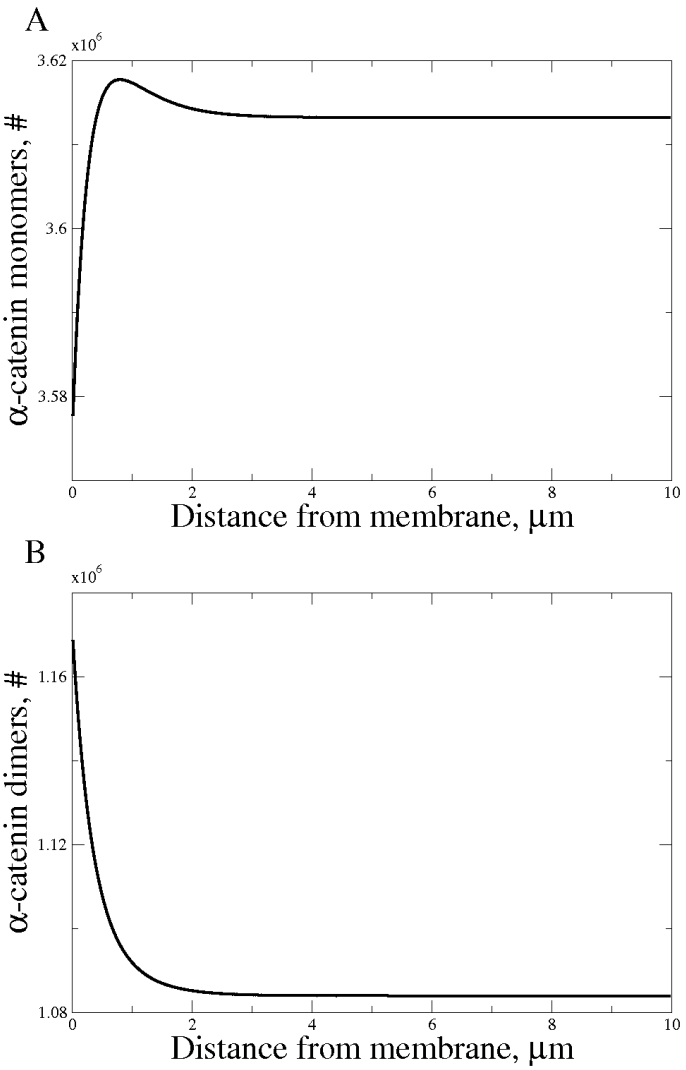
A
x10^6
3.62
3.6
3.58
α-catenin monomers, #
0
2
4
6
8
10
Distance from membrane, μm
B
x10^6
1.16
1.12
1.08
α-catenin dimers, #
0
2
4
6
8
10
Distance from membrane, μm

Figure 6:

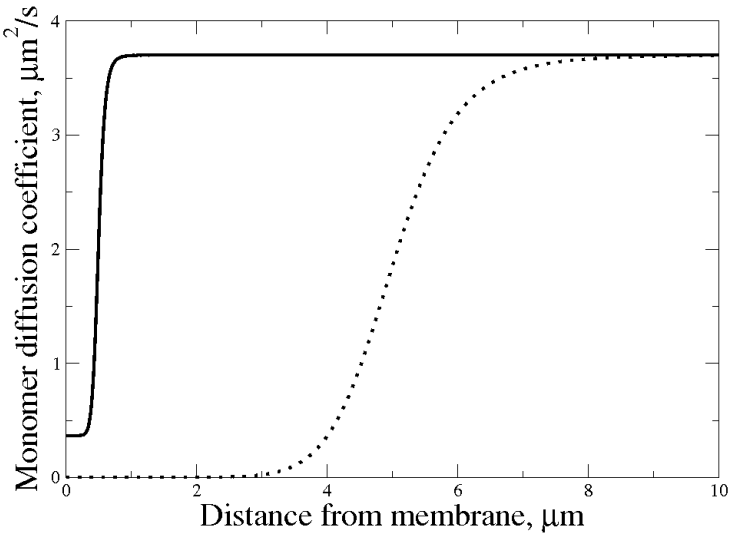
Monomer diffusion coefficient, μm 2/s
Distance from membrane, μm
0
1
2
3
4
0
2
4
6
8
10

Figure 7:

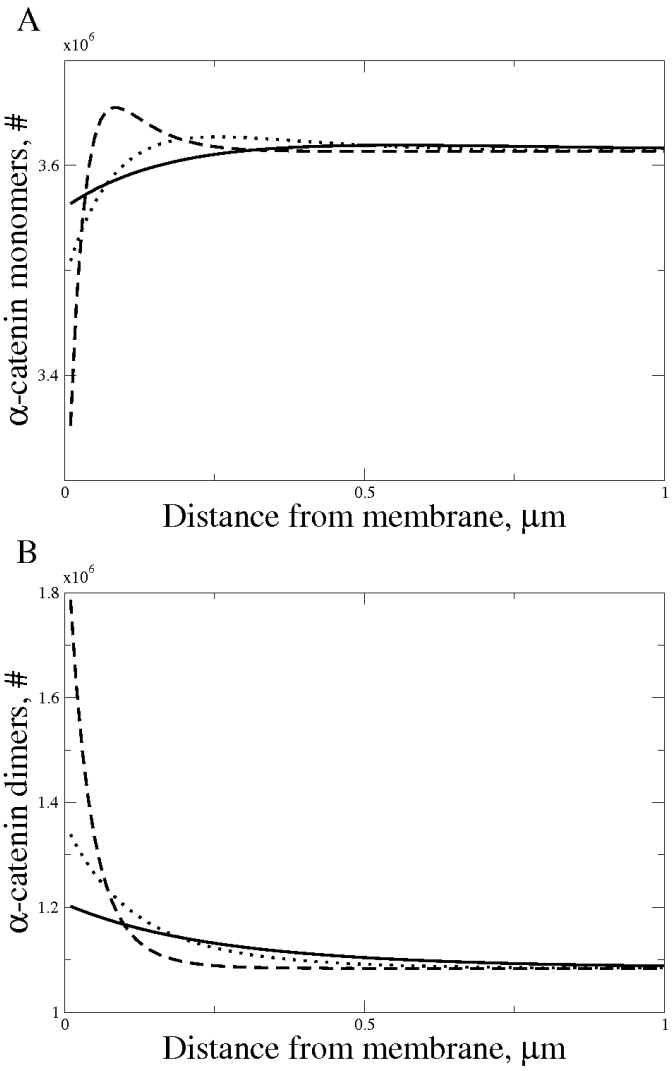
A
x10^6
α-catenin monomers, #
3.6
3.4
0
0.5
1
Distance from membrane, μm
B
x10^6
α-catenin dimers, #
1.8
1.6
1.4
1.2
1
0
0.5
1
Distance from membrane, μm

Figure 8:

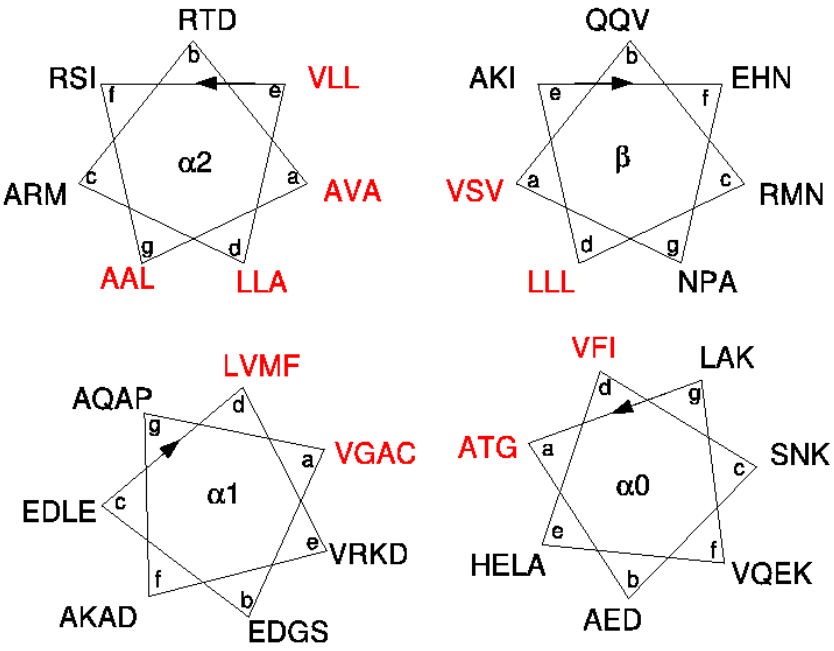
RTD
RSI
VLL
ARM
AVA
AAL
LLA
α2
QQV
AKI
EHN
VSV
RMN
LLL
NPA
β
LVMF
AQAP
VGAC
EDLE
VRKD
AKAD
EDGS
α1
VFI
LAK
ATG
SNK
HELA
VQEK
AED
α0

Figure 9: